Application of a Fully Automatic Autofocusing Algorithm for Post-Processing of Synthetic Aperture Radar Images based on Image Entropy Minimization

A. Malamou[1], A. Karakasiliotis[1], E. Kallitsis[1], G. Boultadakis[1], P. Frangos[1]
[1]Division of Information Transmission Systems and Materials Technology,
School of Electrical and Computer Engineer, National Technical University of Athens,
Iroon Polytechniou St.9, 157 73 Zografou, Athens, Greece
pfrangos@central.ntua.gr

Abstract—In this paper an application of an autofocusing algorithm, previously developed by the authors for the case of Inverse Synthetic Aperture Radar (ISAR) [i.e. airborne radar targets], is presented here for the case of Synthetic Aperture Radar (SAR) geometry [i.e. ground radar targets]. Here, a new theory and methodology for generating SAR synthetic backscattered data is also developed. This algorithm is named 'CPI-split-algorithm', where CPI stands for 'Coherent Processing Interval'. Moreover, two simulation scenarios are presented for a ship target, which is located on the sea surface. In the first simulation scenario, the ship is considered at first to be stationary, and subsequently an oscillatory movement is induced to its position along the vertical axis, due to sea surface motion. In the second simulation scenario, a partial loss of data is examined, caused by temporary accidental malfunctioning of radar transmitter or receiver, assuming that the target (ship) is stationary. Numerical results presented in this paper show the effectiveness of the proposed autofocusing algorithm for SAR image enhancement.

Index Terms—Autofocusing, post processing algorithm, synthetic aperture radar (SAR) imaging.

I. INTRODUCTION

Synthetic aperture radar (SAR) has been widely used as a tool for long-range imaging. This radar is a radio frequency (RF) sensor. Hence, it can perform with high image resolution at long range, regardless the weather conditions, for an airborne or spaceborne radar platform (the former case is examined in this paper). One of its main uses is in target detection and recognition for civilian or military applications. The targets can be either stationary or moving ground objects. Provided that the target remains stationary, the range-Doppler information collected by the SAR antenna leads to the synthesis of the target SAR image with high resolution [1], [2].

As far as moving targets are concerned, the reconstruction of the target image using SAR data is a more difficult task [1]. The SAR image, in this case, is usually degraded by

defocus, distortion or displacement due to target movement. As moving targets are of great interest, the purpose of this paper is to apply the post processing CPI-split autofocusing algorithm [3] for the case of SAR geometry in order to get a focused SAR image of a moving target, as explained below.

Moreover, in order to produce a SAR image, the provided radar data must be of high quality. However in the cases of real-field SAR data, blockages not only due to obstacles or topography, but also because of temporary malfunctioning of radar transmitter or receiver, could lead to partial loss of data. This case of scenario (partial loss of data due to the above reasons) is also examined in this paper, in order to obtain SAR images which are not defective.

II. SIMULATED SAR GEOMETRY AND MATHEMATICAL FORMULATION

The SAR geometry which is used in our simulations is presented in Fig. 1. As it is usual in SAR geometry, the antenna of the radar is assumed to be mounted on a platform such as an aircraft (case of an airborne platform) and the radar illuminates the target during the flight [1]. The aircraft, according to the simulation, travels along positive y-axis, with constant velocity v, along a flight path from $-N/2$ to $N/2$, where N is the number of bursts during one CPI. As it is shown in Fig. 1, the center of the flight path is considered to be point A.
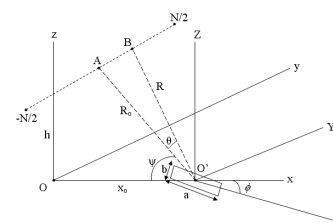

Fig. 1. SAR geometry.

Moreover, the radar antenna is assumed to emit Stepped Frequency (SF) pulses, where M stepped frequencies are emitted per burst ($m = 1$ to M) and N bursts per CPI [1], [2].

The target of observation is a ship located on the sea surface. A 2D geometry of the ship is assumed here, without loss of generality. Hence the dimensions of the ship are: length a and width b. In Fig. 1 two coordinate systems are presented. The coordinate system of the target (ship) to be imaged is called 'local' coordinate system O'XYZ. The other coordinate system is called 'earth' coordinate system Oxyz. The origin O' of the 'local' coordinate system is placed in the mass center of the ship. The distance Ro is the distance between the center of the flight path and the origin O' of the 'local' coordinate system. According to the above geometry the vector of the distance R is given by the following formula

$$\vec{R} = x_o \hat{x} - vnT_b \hat{y} - h\hat{z} \,, \tag{1}$$

where h is the radar platform altitude, $(\hat{x}, \hat{y}, \hat{z})$ are the unit vectors along the (x,y,z) axes respectively, $T_b = M \cdot (PRI)$ is the burst duration (PRI is the Pulse Repetition Interval of the transmitted radar waveform) and n is the burst index ($n = -N/2,...,-1,0,1,2,..., N/2$). The target (ship) is considered to be formed from a set of point scatterers, where in Fig. 2 one of the ship scatterers ($X_{(i,j)}, Y_{(i,j)}$) is shown. The angle ψ is the grazing angle of the incident radar electromagnetic (EM) wave and the angle θ is the azimuthal angle of observation of the target within the CPI. The angle θ is determined by the following equation

$$\cos\theta = \left(\frac{x_o^2 + h^2}{x_o^2 + h^2 + v^2 n^2 T_b^2} \right)^{1/2} . \tag{2}$$
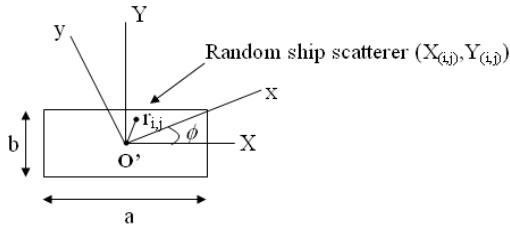

Fig. 2. Position of ship point scatterer (*i,j*).

The total distance from the SAR antenna to an arbitrary ship scatterer is given by the following equation

$$\vec{R}_{i,j} = \vec{R} + [A] \cdot \vec{r}_{i,j} \,, \tag{3}$$

where [A] is the transformation matrix from the 'local' coordinate system to the 'earth' coordinate system

$$A = \begin{bmatrix} \cos\phi & \sin\phi \\ -\sin\phi & \cos\phi \end{bmatrix} \tag{4}$$

and ϕ is the angle between the 'local' and the 'earth' coordinate systems. The angle ϕ also determines the orientation of the ship with respect to the 'earth' coordinate system Oxyz (axis Ox, in particular).

The distance $r_{i,j}$ is the distance between the origin O' of the 'local' coordinate system and an arbitrary ship scatterer and is given by the formula

$$\vec{r}_{i,j} = (X_{i,j}, Y_{i,j}) = X_{i,j} \hat{X} + Y_{i,j} \hat{Y} \,. \tag{5}$$

As a result, combining the above equations, the total distance from the SAR antenna to an arbitrary ship scatterer is given by the formula

$$\vec{R}_{i,j} = \vec{R} + [(X_{i,j} \cos\phi + Y_{i,j} \sin\phi)\hat{x} + (-X_{i,j} \sin\phi + Y_{i,j} \cos\phi)\hat{y}] \,. \tag{6}$$

It can be easily seen that the incident wavevector $\vec{k}$ is given by

$$\vec{k} = k \cos\theta\cos\psi \cdot \hat{x} - k\sin\theta \cdot \hat{y} - k \cos\theta \sin\psi \cdot \hat{z} \,, \tag{7}$$

where θ is given by (2) and k is the wavenumber for the emitted SF waveform

$$k = \frac{\omega_m}{c} = \frac{2\pi f_m}{c} \,, \tag{8}$$

where $f_m = f_o + (m-1)\Delta f \,, (m = 1,2,...,M)$ is the emitted stepped frequency (SF) [1], [2] and ω_m is the corresponding emitted angular frequency.

Hence, the phase $\phi_{i,j}$ for the (*i,j*) scatterer of the target is calculated from analytic (geometric) calculation of the distance $R_{i,j}$ between the radar and the (*i,j*) scatterer of (6), as well as from the analytic expression for the incident wavevector $\vec{k}$ of (7), as follows

$$\phi_{i,j} = 2 \cdot \vec{k} \cdot \vec{R}_{i,j} \,. \tag{9}$$

Then, from (6), (7) and (9) above, the following formula for the 'local scattering phase' is obtained, assuming that the target is stationary

$$\phi_{i,j}^m = \frac{4\pi f_m}{c} [\cos\theta\cos\psi(X_{i,j} \cos\phi + Y_{i,j} \sin\phi) + \\ + \sin\theta \cdot (X_{i,j} \sin\phi - Y_{i,j} \cos\phi), \tag{10}$$

whereas the phase corresponding to distance from position *B* of the platform to the center of the target (ship) *O'* is compensated by the radar processor during SAR image synthesis [see also (1)]

$$\phi_{i,j}^m = \frac{4\pi f_m}{c} (x_o \cos\theta\cos\psi + h \cos\theta \sin\psi + vnT_b\sin\theta) \,. \tag{11}$$

Furthermore, m is the stepped frequency index ($m = 1,...,M$); n is the burst index ($n = 1,..., N \cdot N_{CPI}$) for a number of simulated CPI's (N_{CPI}); N is the number of bursts during one CPI and ($X_{(i,j)}, Y_{(i,j)}$) are the local coordinates of the ship scatterers.

In the case of a moving target which is examined here, the ship is supposed to have a vertical movement due to the sea surface motion and, as a result, the phase formula changes accordingly. In this particular ship motion model, an extra term is added due to the ship movement along the *z*-axis and

it depends on the period T_{osc} of the sea surface motion. Hence, the phase of the backscattered signal is given by

$$\phi_{i,j,osc}^{m} = \phi_{i,j}^{m} - \frac{4\pi f_m}{c} z_o \cos\theta \sin\psi \sin(\omega_{osc} t), \qquad (12)$$

where z_0 is the oscillation amplitude and ω_{osc} is the angular frequency of the oscillation ($\omega_{osc} = 2\pi / T_{osc}$).

Then, the backscattered radar data are simulated through the following formula

$$x(m,n) = \sum_d s_{i,j} \exp[j\phi_{i,j}^{m}] + u(m,n), \qquad (13)$$

where d is the number of the scatterers of the target and $s_{i,j}$ is the scattering intensity for the (i,j) scatterer. In the simulations below we can assume, without loss of generality, that all scatterers have the same strength in amplitude ($s_{i,j} = 1$ for all i,j). The term $\phi_{i,j}$ is the phase of the backscattered signal (10) or (12), while $u(m,n)$ is the two dimensional additive white Gaussian noise component.

In the numerical simulations below, the raw data matrices are formed through (13). It is worthy to mention, that the dependence on 'slow – time' index n in (10) and (12) becomes effective through the aspect angle θ, see (2).

The SAR images for all CPI's are constructed from the raw data matrices through the traditional 'Range – Doppler' imaging technique, involving FFT processing in both range and Doppler directions [2]. In order to compare the quality of the SAR images obtained, the entropy value of each image is computed, which corresponds to the SAR image quality as a comparison criterion [3], [4].

III. FAST MANEUVERING TARGET SIMULATION SCENARIO – NUMERICAL RESULTS

In the first simulation scenario, the ship is considered in most CPI's of observation to be stationary. Subsequently in some specific CPI's, an oscillatory movement is induced to its position along the vertical z-axis, due to sea surface motion. The SAR images that are obtained for these CPI's are blurred due to the ship movement, which effect is removed by our proposed autofocusing algorithm [3].
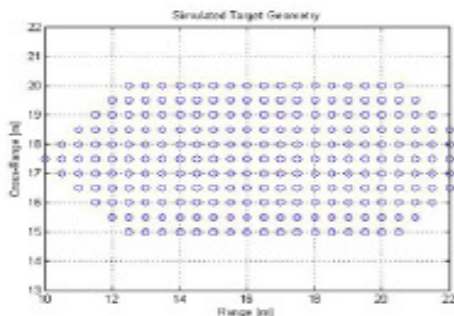

Fig. 3. Geometry of the simulated ship target (in all Fig. 3 to Fig. 6 horizontal axis is 'range direction', while vertical axis is 'cross range direction', see text).

The simulated ship geometry is shown in Fig. 3. It is a point scatterer model which consists of 233 scatterers. The corresponding radar and geometry parameters are shown in Table I. Note here that through suitable selection of these parameters 'square resolution' of SAR images is obtained [4].

TABLE I. SAR SIMULATION PARAMETERS.

Parameter	Value [units]
carrier frequency, f_0	10 [GHz]
radar bandwidth, B	300 [MHz]
number of frequencies, M	64
pulse repetition frequency, PRF	2.74 [KHz]
burst duration, T_b	0.0234 [s]
coherent processing interval, CPI	3 [s]
number of bursts, N	128
number of CPIs, N_{CPI}	13
range distance to center of target, R_0	10 [km]
height of SAR platform, h	2 [km]
position angle of the ship, φ	0°
velocity of platform, v	100 [m/s]
oscillation amplitude, z_0	0.2 [m]
oscillation period, T_{osc}	1.3 [s]

In this simulation, the flight duration is considered to be 13 CPI's. The ship movement is induced only in the 4th and 8th CPI. In Fig. 4 the produced SAR images for the 1st and 13th CPI are presented. In this figure, as well as in all Fig. 3 to Fig. 6, the horizontal axis represents the 'range direction' (direction of propagation of radar waves, axis Ox in Fig. 1), while the vertical axis represents the 'cross – range direction' (or 'along track direction', axis Oy in Fig. 1) [1]–[6]. It can be easily noticed that there is a change in the angle of observation as the SAR antenna moves along the flight path.

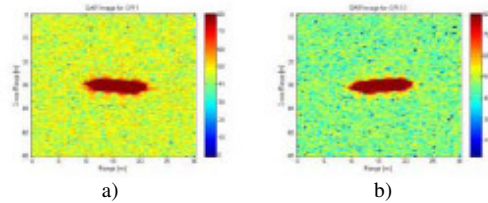
a)   b)

Fig. 4. SAR images for the 1st and 13th CPI.

The CPI-split autofocusing algorithm is employed in those CPI's which entropy values exceed a threshold that represents an acceptable SAR image quality [3]. The images with entropy values below the entropy threshold are called "focused" images, while the images with entropy values over the threshold are called "unfocused". It is expected that the SAR images which correspond to those specific CPI's in which the ship movement is induced, will have greater entropy values than the SAR images corresponding to no ship movement. In this simulation scenario the value of the entropy threshold was set equal to 6.0 [3].

In Fig. 5, four SAR images are presented. Images 5 (a), 5 (b) and 5 (c) represent the reconstructed SAR images for the 3rd, 4th and 5th CPI respectively. It is clear that the SAR image of the 4th CPI (image 5 (b)) is unfocused due to sea motion, as modeled in our simulations. In image 5 (d) the SAR image of the 4th CPI is shown after the application of the CPI-split autofocusing algorithm [3]. Clearly the SAR image is now focused and has an acceptable entropy value. Similar results are obtained for the case of the 8th CPI [7].
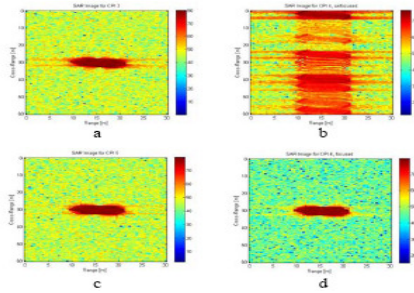
Fig. 5. Reconstructed SAR images for the a) 3rd, b) 4th, c) 5th CPI, d) the 4th CPI after application of the CPI-split algorithm.

In Table II the entropy values for the CPI's related to the application of the algorithm are presented. Note that the entropy values of the 4th CPI are within the acceptable entropy value range (e.g. below the entropy threshold), after our proposed algorithm is applied [3].

TABLE II. ENTROPY VALUES OF THE SAR IMAGES.

SAR Image	Entropy	Minimum Entropy Combination
3rd CPI	5.7583	
4th CPI, unfocused	7.7692	
5th CPI	5.7624	
4th CPI, focused	5.758	stage 4, segment 2, combination 7 [3]

IV. PARTIAL LOSS OF DATA SIMULATION SCENARIO – – NUMERICAL RESULTS

Regarding the second simulation scenario, a partial loss of data is simulated in some specific CPI's, due, for example, to accidental malfunctioning of the radar transmitter or receiver during that time period. The same simulated ship geometry as in Fig. 3 is used. The main idea also for this simulation scenario is to apply the CPI-split autofocusing algorithm [3] in order to produce SAR images of the target that have good quality despite the partial loss of data. For these specific CPIs, the backscattered signal during the partial loss of data is considered to be zero, and only the two dimensional additive white Gaussian noise component $u(m,n)$ is taken into account.

The corresponding radar and geometry parameters are considered to be the same as in the previous simulation (Table 1). In this simulation, the flight duration is considered to be 13 CPI's. The data loss occurs, according to the simulation, only in the 4th and 8th CPI. Our proposed CPI – split autofocusing algorithm is applied, in a way similar to Section III, above, with selected threshold for entropy value equal to 6.0.

In Fig. 6, four SAR images are presented. Images 6 (a), 6 (b) and 6 (c) represent the reconstructed SAR images for the 7th, 8th and 9th CPI respectively. It is clear that the SAR image of the 8th CPI [image 6 (b)] is defective due to the bad data transmission or reception, as modelled in our simulations. In image 6 (d) the SAR image of the 8th CPI is shown after the application of the CPI-split autofocusing algorithm [3]. Clearly the SAR image is now focused and has an acceptable entropy value. The CPI-split autofocusing algorithm is effective also in this simulation scenario. Similar results were obtained for the 4th CPI (not shown here). In Table III the entropy values are presented.
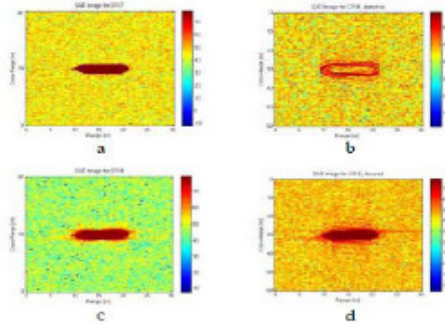

Fig. 6. Reconstructed SAR images for the a) 7th b) 8th c) 9th CPI and d) the 8th CPI after application of the CPI-split algorithm

TABLE III. ENTROPY VALUES OF THE SAR IMAGES.

SAR Image	Entropy	Minimum Entropy Combination
7th CPI	5.6533	
8th CPI, defective	7.7074	
9th CPI	5.7263	
8th CPI, focused	5.7772	stage 3, segment 2, combination 3 [3]

V. CONCLUSIONS

In this paper, the 'CPI-split autofocusing algorithm' [3] is applied to two different Synthetic Aperture Radar (SAR) scenarios, namely for the case of moving target (ship) in vertical (z) axis because of sea surface motion, and for the case of partial loss of data at radar transmitter or receiver. The application of our proposed algorithm produced excellent focusing of SAR images for both cases, above.

Regarding near future related research by our group, this includes to examine simulation results for three-dimensional ship representation, as well as for more complicated ship motion (in roll, yaw and pitch). Furthermore, to examine the cases of moving ship target with constant velocity on the sea surface, as well as the case of spaceborne SAR platform (instead of the case of airborne SAR platform examined in this paper). Finally, to incorporate the proposed 'CPI-split autofocusing algorithm' also for the case of real field radar data.

REFERENCES

[1] D. Wehner, *High-Resolution Radar*, London, Artech House, 2nd ed., 1995.

[2] V. Chen, H. Ling, *Time-Frequency Transforms for Radar Imaging and Signal Analysis*. London, Artech House, 2002.

[3] E. Kallitsis, A. Karakasiliotis, G. Boultadakis, P. Frangos, "A Fully Automatic Autofocusing Algorithm for Post-processing ISAR Imaging based on Image Entropy Minimization", *Elektronika ir Elektrotechnika (Electronics and Electrical Engineering)*, no. 4, pp. 125–130, 2011.

[4] A. Lazarov, C. Minchev, "ISAR Signal Modeling and Image Reconstruction with Entropy Minimization Autofocusing", in *Proc. of DASC*, Portland, USA, 2006, pp. 3E5-1–3E5-11.

[5] J. Li, R. Wu, V. Chen, "Robust autofocus algorithm for ISAR imaging of moving", *IEEE Trans. Aerosp. Electron. Syst.*, vol. 37, no 3, pp. 1056–1069, 2001. [Online]. Available: http://dx.doi.org/ 10.1109/7.953256

[6] D. Pastina, A. Farina, J. Gunning, P. Lombardo, "Two-dimensional super resolution spectral analysis applied to SAR images", *IEE Proc.*, Radar Sonar Navig., vol. 145, no 5, pp. 281–290, 1998. [Online]. Available: http://dx.doi.org/10.1049/ip-rsn:19982225

[7] A. Malamou, A. Karakasiliotis, E. Kallitsis, G. Boultadakis, P. Frangos, "An autofocusing algorithm for post-processing of synthetic aperture radar (SAR) images based on image entropy minimization", in *Proc. of International Conference CEMA 12*, Athens, Greece, 2012, pp. 53–56.